

Cospectral budget of turbulence explains the bulk properties of smooth pipe flow

*Original*

Cospectral budget of turbulence explains the bulk properties of smooth pipe flow / Katul, Gabriel George; Manes, Costantino. - In: PHYSICAL REVIEW E, STATISTICAL, NONLINEAR, AND SOFT MATTER PHYSICS. - ISSN 1539-3755. - STAMPA. - 90:6(2014). [10.1103/PhysRevE.90.063008]

*Availability:*

This version is available at: 11583/2624419 since: 2015-12-17T15:25:57Z

*Publisher:*

AMERICAN PHYSICAL SOC, ONE PHYSICS ELLIPSE, COLLEGE PK, USA, MD, 20740-3844

*Published*

DOI:10.1103/PhysRevE.90.063008

*Terms of use:*

This article is made available under terms and conditions as specified in the corresponding bibliographic description in the repository

*Publisher copyright*

(Article begins on next page)

# Bottlenecks in turbulent kinetic energy spectra predicted from structure function inflections using the Von Kármán-Howarth equation

Gabriel G. Katul,<sup>1,2</sup> Costantino Manes,<sup>3</sup> Amilcare Porporato,<sup>1,2</sup> Elie Bou-Zeid,<sup>4</sup> and Marcelo Chamecki<sup>5</sup>

<sup>1</sup>Nicholas School of the Environment, Box 80328, Duke University, Durham, North Carolina 27708, USA

<sup>2</sup>Department of Civil and Environmental Engineering, Duke University, Durham, North Carolina 27708, USA

<sup>3</sup>Faculty of Engineering and the Environment, University of Southampton, Southampton, SO171BJ, UK

<sup>4</sup>Department of Civil and Environmental Engineering, Princeton University, Princeton, New Jersey 08544, USA

<sup>5</sup>Department of Meteorology, Pennsylvania State University, University Park, Pennsylvania 16802, USA

(Received 26 January 2015; published 11 September 2015)

The compensated three-dimensional turbulent kinetic energy spectrum exhibits a peculiar bump at wave numbers in the vicinity of the crossover from inertial to viscous regimes due to pile up in turbulent kinetic energy, a phenomenon referred to as the *bottleneck effect*. The origin of this bump is linked to an inflection point in the second-order structure function in physical space caused by competition between vortex stretching and viscous diffusion mechanisms. The bump location and magnitude are reasonably predicted from a novel analytical solution to the Von Kármán-Howarth equation reflecting the competition between these two mechanisms and accounting for variable structure skewness with decreasing scale.

DOI: [10.1103/PhysRevE.92.033009](https://doi.org/10.1103/PhysRevE.92.033009)

PACS number(s): 47.27.nb

## I. INTRODUCTION

At wave numbers  $k$  much larger than the integral length scale of the flow ( $L_p$ ), the three-dimensional turbulent kinetic energy spectrum  $\phi_{tke}(k)$  exhibits a “bottleneck” whose signature is a bump at the crossover from inertial to viscous regimes in its compensated form  $k^{5/3}\phi_{tke}(k)$ . This “bump” has been confirmed by direct numerical simulations (DNS), experiments, and theories including the Test Field Model (TFM) and Eddy-Damped Quasi-Normal Model (EDQNM) [1–13]. Not accounting for the bottleneck prevents acceptable reproduction of the longitudinal velocity gradient skewness [10,14,15] thereby prompting interest in phenomenological theories that explain the onset of such a bottleneck and provide mathematical representation of the shape of  $\phi_{tke}(k)$  around the bottleneck. It is for this reason that the causes of the bottleneck received scrutiny [6,12,16,17]. One study attributes the bottleneck occurrence entirely to the restricted inertial subrange in DNS [18]. Models based on TFM and EDQNM propose the main source of energy in the bump to be nonlocal interactions governing the transfer terms across the energy cascade [2]. On similar theoretical lines, it is accepted that the bottleneck arises due to the lack of small-scale vorticity at  $k$  exceeding the so-called Kolmogorov microscale wave number  $k_d \propto \eta^{-1}$ , where  $\eta = (\nu^3/\epsilon)^{1/4}$  is the smallest length scale of turbulence where the action of fluid viscosity ( $\nu$ ) is appreciable and  $\epsilon = 2\nu \int_0^\infty k^2 \phi_{tke}(k) dk$  defines the mean turbulent kinetic energy dissipation rate, which is assumed to be identical to the energy transfer rate across scales. In the vicinity of  $k_d$ , absence of small-scale vortices makes this energy cascade less efficient thereby resulting in an apparent energy pileup in  $\phi_{tke}(k)$  for  $k < k_d$ . The bottleneck effect was shown to be amplified when unrealistic hyperviscosity was used in simulations [3,5,7,8,11,17]. However, this bottleneck appears much weaker [4,19,20] or almost absent [1,21] in many experiments reporting one-dimensional component-wise velocity spectra, at least compared to DNS results reporting three-dimensional  $\phi_{tke}(k)$ . The reason for the presence of a bottleneck in three dimensions but their muted or

absent signature in one-dimensional component-wise spectra is understood [1,7]. What is contested is the level of complexity needed to reproduce the main features of the bottleneck. Bumps at the crossover from large scales to inertial scales have also been reported and discussed [6], but they are beyond the scope of the work here. Previous approaches were based on complex two-point closure schemes used to predict the evolution of  $\phi_{tke}(k)$  usually from the Von Kármán-Howarth (VKH) equation written in spectral space (e.g., the EDQNM and TFM closure schemes mentioned above) since their applicability extends beyond inertial range scales. It is demonstrated here that the bottleneck can be analytically predicted from the VKH equation [13,22–24] written in physical rather than spectral space using a closure scheme that accommodates variable structure skewness approximation across scales. While the VKH modeled second-order structure function  $D_2(r)$  with scale  $r$  does not exhibit a bottleneck, the bump in the compensated turbulent kinetic energy spectrum is linked to a maximum in  $r^{1/3}dD_2(r)/dr$ , which approximately coincides with an  $r$  at which  $d^2D_2(r)/dr^2 = 0$ . The  $d^2D_2(r)/dr^2 = 0$  is an outcome of a competition between vortex stretching and viscous diffusion mechanisms.

## II. DEFINITIONS

In homogeneous isotropic turbulence, the  $n$ th-order structure function of a turbulent velocity component  $q = u, v, w$  with variance  $\sigma_q^2 = \sigma_u^2 = \sigma_v^2 = \sigma_w^2$  and turbulent kinetic energy  $(3/2)\sigma_q^2$  at two points separated by distance  $r$  is given by

$$D_n(r) = \langle (\Delta_r q)^n \rangle, \quad (1)$$

where  $\Delta_r q$  defines the differences in the flow variable  $q$  at two points in the fluid separated by a scalar distance  $r$ ,  $r = (r_x^2 + r_y^2 + r_z^2)^{1/2}$ ,  $r_x$ ,  $r_y$ , and  $r_z$  are separation distances projected along the longitudinal ( $x$ ), lateral ( $y$ ), and vertical ( $z$ ) directions, respectively, and  $u$ ,  $v$ ,  $w$  are velocity components along  $x$ ,  $y$ ,  $z$  and  $\langle \cdot \rangle$  is ensemble averaging. The  $D_2(r)$  is related

to  $\phi_{tke}(k)$  using [6,25]

$$D_2(r) = \frac{4}{3} \int_0^\infty \left[ 1 - \frac{\sin(kr)}{kr} \right] \phi_{tke}(k) dk, \quad (2)$$

where  $k = (k_x^2 + k_y^2 + k_z^2)^{1/2}$ . At  $r \geq L_p$ ,  $D_2(r) \approx 2\sigma_q^2 \approx (4/3) \int_0^\infty \phi_{tke}(k) dk$ . Also, as  $r \rightarrow 0$ ,  $\sin(kr)/(kr) \rightarrow 1$  and  $D_2(0) \rightarrow 0$  irrespective of the shape of  $\phi_{tke}(k)$  as expected from its definition. An inflection point in  $D_2(r)$  is necessary but not sufficient for explaining a bump in  $\phi_{tke}(k)$  as shown elsewhere [6]. The main mechanisms causing this inflection point and why they can lead to a bump in  $\phi_{tke}(k)$  are now discussed in the context of the VKH equation.

### III. THE VON KÁRMÁN–HOWARTH (VKH) EQUATION

Prior results [13,23] and numerical studies [9] demonstrated connections between solutions to VKH (in physical space) and  $\phi_{tke}(k)$ . A logical starting point for developing a phenomenological theory is the simplest form of the VKH equation in physical space that retains all the essential mechanisms at the crossover from inertial to viscous regimes. For simplicity,  $q = u$ , the turbulent kinetic energy is  $(3/2)\sigma_u^2$ , and the VKH equation for the  $u$  component is given by

$$D_3(r) - 6\nu \frac{dD_2(r)}{dr} = -\frac{4}{5}\epsilon r, \quad (3)$$

where the right-hand side is the net energy transfer rate cascading from scale  $r$  to finer scales,  $D_3(r)$  is inertial cascade related to generation of enstrophy by vortex-line stretching ( $D_3(r) \sim r^3 \langle \omega_i(r) \omega_j(r) S_{ij}(r) \rangle$ , where  $\omega$  is vorticity and  $S_{ij}$  is the strain rate [23]) and  $6\nu dD_2(r)/dr$  is the removal rate by viscous diffusion. In the limit of  $6\nu dD_2(r)/dr \rightarrow 0$ , Eq. (3) recovers the well-known  $D_3(r) = \langle [u(x+r) - u(x)]^3 \rangle = -(4/5)\epsilon r$  or the so-called Kolmogorov's 4/5 rule [26]. It also implies that when viscous diffusion is negligible, as is the case in the inertial subrange, vortex stretching is responsible for much of the net energy transfer rate at scale  $r$ . When interpreting  $D_2(r)$  as representing the squared amplitude of the mean velocity gradient at scale  $r$  [i.e.,  $D_2(r) \sim \langle (r du/dr)^2 \rangle$ ], the VKH equation can be physically translated into a competition between vortex stretching [i.e.,  $D_3(r)$ ] and viscous diffusion [i.e.,  $\nu dD_2(r)/dr$ ] mechanisms to match energy dissipation [i.e.,  $-(4/5)\epsilon r$ ]. On the one hand, the viscous diffusion term “smooths out” velocity gradients (and hence vorticity) at scale  $r$ . On the other hand, velocity gradients do contribute to  $D_3(r) \sim r^3 \langle \omega_i(r) \omega_j(r) S_{ij}(r) \rangle$  to efficiently transfer energy from  $r$  to finer scales thereby setting up the competing mechanisms.

### IV. CLOSURE SCHEMES

To predict  $D_2(r)$ , closure approximations to the vortex stretching term are necessary and wide-ranging possibilities exist [24]. Using the constant skewness hypothesis as a closure of maximum simplicity [27],  $D_3(r) = S_u D_2(r) |D_2(r)|^{1/2}$ . The constant structure skewness  $S_u$  value can be determined from inertial subrange scaling by noting that  $D_2(r) \approx C'_k \epsilon^{2/3} r^{2/3}$  resulting in  $S_u \approx -(4/5)/(C'_k)^{3/2} \approx -0.27$ , where  $C'_k = (4/3)C_k = 2.0$  is the Kolmogorov constant associated with the second-order structure function (in three dimensions).

With a constant  $S_u$ , Eq. (3) reduces to [23]

$$\frac{dD_2(r)}{dr} + a_u D_2(r) |D_2(r)|^{1/2} = b_u r, \quad (4)$$

where  $a_u = -S_u/(6\nu)$  and  $b_u = (2/15)(\epsilon/\nu)$ . A point of departure from earlier work [23] is to obtain an analytical solution of Eq. (4) while retaining a *variable structure skewness* for scales smaller than those in the inertial subrange. A variable structure skewness can be achieved by assuming a linear relation between  $D_3(r)$  and  $D_2(r)$  given as  $D_3(r) = S_u (C'_k \epsilon^{2/3} r^{2/3})^{1/2} D_2(r)$ . This simplification is arbitrary but accommodates the numerous experiments and simulations [9,13] that demonstrated the structure skewness computed as  $-D_3(r)[D_2(r)]^{-3/2}$  increases with decreasing  $r$  outside the inertial subrange. With this approximation, Eq. (4) simplifies to

$$\frac{dD_2(r)}{dr} + a'_u D_2(r) r^{1/3} = b_u r, \quad (5)$$

where  $a'_u = a_u (C'_k)^{1/2} \epsilon^{1/3}$  recovers the Kolmogorov scaling in the inertial subrange for  $D_2(r)$ . This equation captures the competition between a nonlinear vortex stretching and a linear viscous diffusion and can be analytically solved when enforcing  $D_2(0) = 0$  to yield a compact expression given by

$$\frac{D_2(r)}{C'_k (\epsilon r)^{2/3}} = 1 - \frac{1}{\frac{1}{2} \sqrt{3} a'_u r^{2/3}} \text{Daw}_F \left( \frac{1}{2} \sqrt{3} a'_u r^{2/3} \right), \quad (6)$$

where  $\text{Daw}_F(\zeta)$  is the Dawson function given by

$$\begin{aligned} \text{Daw}_F(\zeta) &= \exp(-\zeta^2) \int_0^\zeta \exp(p^2) dp \\ &\approx \zeta - \frac{2}{3}\zeta^3 + \frac{4}{15}\zeta^5 - \frac{8}{105}\zeta^7 + \dots \end{aligned} \quad (7)$$

Equation (6) can be arranged to yield

$$\frac{D_2(r)}{C'_k (\epsilon r)^{2/3}} = y_c(\zeta) = 1 - \frac{1}{\zeta} \text{Daw}_F(\zeta), \quad (8)$$

where  $\zeta = \theta(r/\eta)^{2/3}$ ,  $\theta = (10C'_k)^{-1/2}$ , and  $y_c$  is a nondimensional second-order structure function. Figure 1 shows that Eq. (8) reasonably approximates a numerical solution to Eq. (4) that employs a constant structure skewness [23]. Figure 2 compares the structure skewness predicted from the analytical solution here  $\approx -0.27[1 - \frac{1}{\zeta} \text{Daw}_F(\zeta)]^{-1/2}$ , the constant skewness assumption  $S_u \approx -0.27$ , and the measured structure skewness reported elsewhere [13]. It is clear that the constant skewness model (numerical) and the variable skewness analytical solution proposed here bound expected variations in structure skewness with decreasing  $r$ . It follows that any agreement between these two modeled outcomes can be viewed as a robustness measure to the precise skewness closure (constant or dynamic across scales). As a further check, good agreement was found between Eq. (8) and the Batchelor scaling for  $D_2(r)$  described elsewhere [6]. The Batchelor scaling was demonstrated to be robust to finite Reynolds number and large-scale anisotropic effects than its spectral counterpart when identifying the crossover from inertial to viscous ranges [6]. The viscous diffusion term causes deviations from K41 scaling through the Dawson function that then introduces an inflection point in  $D_2(r)$ . As expected, when

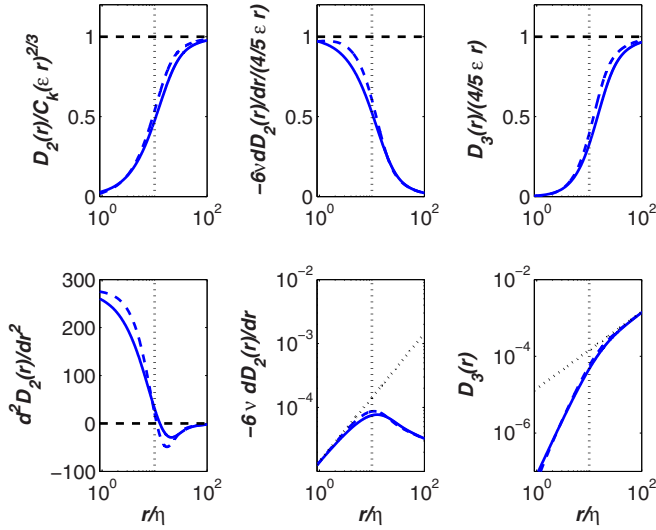


FIG. 1. (Color online) Top: Comparison between the analytical (solid, variable structure skewness) and numerical (dashed, constant structure skewness) solutions to  $y_c$  and the competing terms in the VKH equation. The comparison suggests that  $y_c(\zeta) = 1 - \zeta^{-1}\text{Daw}_F(\zeta)$  reasonably approximates the VKH equation and all its terms in the inertial to viscous ranges when closed with  $S_u \approx -0.27$ . Dimensionless (top panels) and dimensional (bottom panels) results are shown with  $-(4/5)\epsilon r$  highlighted in the bottom-center and -right panels. Note the inflection point in  $D_2(r)$  at scale  $r/\eta \in [5, 10]$  determined by  $d^2 D_2(r)/dr^2 = 0$  (bottom left).

$r/\eta \gg 1$ , vortex stretching [i.e., modeled  $D_3(r)$ ] explains much of the  $(4/5)\epsilon r$  term, and conversely, when  $r/\eta \sim 1$ , viscous diffusion explains the remaining  $(4/5)\epsilon r$  around the Kolmogorov microscale  $\eta$  (top-mid and top-right panels in Fig. 1). In the vicinity of  $r/\eta = 5 - 10$ , the analytical solution with its variable structure skewness and the numerical solution with its constant structure skewness confirm the occurrence of a maximum in the viscous diffusion term coinciding with an inflection point in  $D_2(r)$  [i.e.,  $d^2 D_2(r)/dr^2 = 0$ ]. This is the scale where the spectral bottleneck peak is expected. It follows that an occurrence of a maximum in the viscous diffusion term, analytically and numerically predicted to occur at some scale  $r/\eta \in [5, 10]$  irrespective of the skewness closure, must also coincide with the scale that most effectively weakens the efficiency of vortex stretching with further reductions in  $r$  [i.e., the term  $dD_3(r)/dr = -(4/5)\epsilon - 6vd^2 D_2(r)/dr^2$ ]. The term  $6vd^2 D_2(r)/dr^2$  reverses sign with reduced  $r$  at  $r/\eta \in [5, 10]$  while  $(4/5)\epsilon$  remains constant. This turns out to be the link with the spectral bottleneck commonly featured as a bump in  $k^{5/3}\phi_{tke}(k)$  as will be seen in the next section.

## V. THE SPECTRAL BUMP

It was shown that in physical (or  $r$ ) and spectral (or  $k$ ) spaces, the kinetic energy of eddies of size  $\eta < r = l_e < L_p$  are approximately [23]

$$rV(r)|_{r=l_e} \approx [k\phi_{tke}(k)]_{k=\hat{\pi}/l_e}; V(r) = -\frac{3}{8}r^2 \frac{d}{dr} \frac{1}{r} \frac{dD_2(r)}{dr}, \quad (9)$$

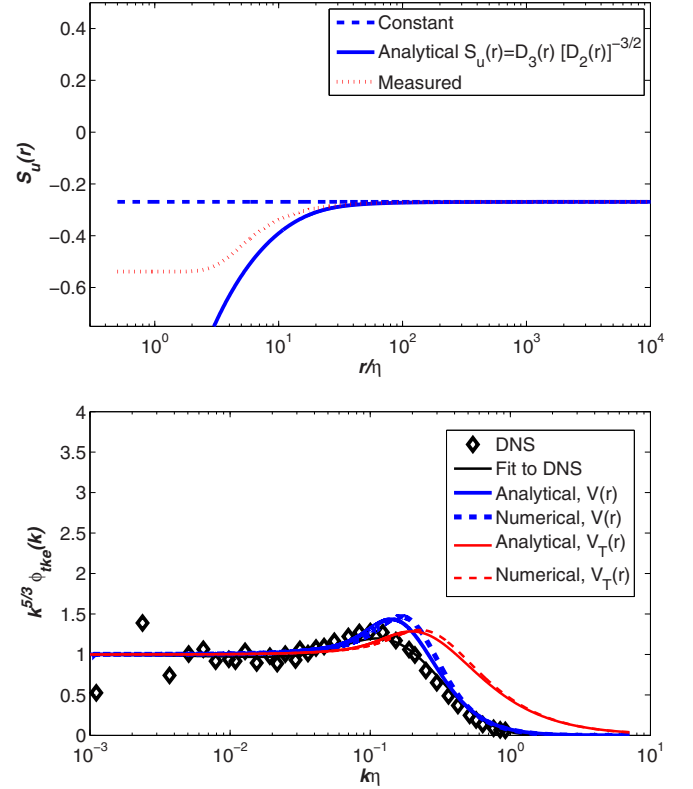


FIG. 2. (Color online) Top: Measured variations in  $S_u(r)$  (dot) relative to the constant (dashed)  $S_u = -0.27$  and modeled  $\approx -0.27[1 - \frac{1}{\zeta}\text{Daw}_F(\zeta)]^{-1/2}$  using the analytical solution to the VKH. Bottom: Comparison between DNS reported  $k^{5/3}\phi_{tke}(k)$  reported elsewhere [10] along with modeled  $k^{5/3}\phi_{tke}(k)$  from the VKH (analytical and numerical) equation with  $D_2(r)$  transformed to the Fourier domain using Eq. (9). DNS results from other studies [15] are also included as symbols. For reference, modeled  $k^{5/3}\phi_{tke}(k)$  using  $V_T(r)$  are featured.

where  $\hat{\pi} = 9\pi/8$  and  $V(r)$  is the signature function. The  $rV(r)$  approximation to  $k\phi_{tke}(k)$  breaks down in the vicinity of  $r = \eta$  but holds reasonably far from it (i.e., around the presumed location of the bottleneck). Numerical experiments were conducted (not shown) and confirm that estimating  $\phi_{tke}(k)$  from  $\phi_{tke}(k) = k^{-1} \int_0^\infty \sin(kr)(dD_2(r)/dr)dr$  reasonably agree with Eq. (9) in the inertial subrange and in the vicinity of the bottleneck though these numerical experiments suffer from the finite size corrections discussed elsewhere [6]. Using the  $V(r)$  approximation, some distortion of  $\phi_{tke}(k)$  become significant for  $k\eta > 0.2$ . The scaling analysis between  $k$  and  $r$  spaces is now exploited to identify the bump location given by  $d[k^{5/3}\phi_{tke}(k)]/dk = 0$  or the equivalent  $r$  location where  $d[r^{1/3}V(r)]/dr = 0$ . Inserting the analytical result for  $D_2(r)$  into  $V(r)$  leads to an  $r$  that satisfies  $d[r^{1/3}V(r)]/dr = 0$  obeying the algebraic equation

$$-5C'_k \left(\frac{r}{\eta}\right)^{2/3} + \left[5C'_k + \left(\frac{r}{\eta}\right)^{4/3}\right] G(r/\eta) = 0, \quad (10)$$

where  $G(r/\eta) = \sqrt{10}\text{Daw}_F[(r/\eta)^{2/3}/\sqrt{10C'_k}]$ . An approximate solution to Eq. (10) corresponds to  $r/\eta = (10C'_k)^{3/4}$ . For  $C'_k = 2$ , this leads to a bottleneck at  $r/\eta = 10$ , which is close

to the  $r/\eta$  at which  $d^2 D_2(r)/dr^2 = 0$ . The predicted bump location and magnitude are now compared with DNS results reporting  $k^{5/3} \phi_{tke}(k)$ . When the entire spectrum is estimated from Eq. (9) and Eq. (6), agreement between DNS results and model calculations shown in Fig. 2 is encouraging except close to  $k\eta = 1$  (as expected). Again, it must be emphasized that the DNS results do have their own limitations and suffer from finite-size effects and some large-scale anisotropy due to finite shearing [6], which are absent from the VKH model. The outcome of the numerical solution with constant skewness closure to the VKH equation shown in Fig. 1 is presented to illustrate that the findings are not sensitive to such skewness closure. Also, the same analysis is repeated with a Townsend  $V_T(r) = (3/4)dD_2(r)/dr$  and the main conclusions about the occurrence and magnitude of the spectral bump are not significantly altered even though distortions to predicted  $k^{5/3} \phi_{tke}(k)$  in the viscous range are larger as foreshadowed by other studies [6]. Hence, the presence of a viscous diffusion term ensures the existence of an inflection point in  $D_2(r)$  or a maximum in  $dD_2(r)/dr$ , which is one of the agents necessary to cause a bump in  $k^{5/3} \phi_{tke}(k)$  when employed with Eq. (10). The inflection point in  $D_2(r)$  appears necessary for the onset of a spectral bump but clearly not sufficient. An inflection in the *compensated and normalized structure function* given by  $W_n(r) = (1 - \gamma_c)\zeta$  can delineate the onset of a spectral bottleneck [unlike  $D_2(r)$ ]. For the analytical solution to the VKH proposed here with a variable structure skewness,  $W_n(r)$  possess an inflection point as predicted from Eq. (8) by virtue of  $Daw_F(\zeta)$  shape that also coincides with the inflection point in  $D_2(r)$ . On the other hand, a spectrum of the form  $\phi_{tke}(k) = C\epsilon^{2/3}k^{-5/3} \exp(-\alpha k\eta)$ , when transformed into physical space using Eq. (9), yields a  $D_2(r)$  that has an

inflection point; however, it can be shown that the  $W_n(r)$  of  $D_2(r)$  associated with this spectrum does not possess an inflection point even though  $D_2(r)$  has an inflection point. This is the sought result.

## VI. CONCLUSION

Simple (i.e., algebraic) closure schemes previously adopted to integrate spectral-budget equations (e.g., Heisenberg or Pao's hypothesis) [23] fail to reproduce the bottleneck effect observed in compensated spectra and were replaced by much more complex approaches such as the TFM and EDQNM closure scheme. This level of complexity is not required when working in real space. An analytical model that accommodates decreased structure skewness with decreasing scale used in conjunction with the VKH equation reasonably predicted the spectral bump location and magnitude. It also compares reasonably with the Batchelor scaling for  $D_2(r)$  in physical space, where the crossover from inertial to viscous is shown to be robust to large-scale anisotropy and finite-size effects [6] than its spectral counterpart. As pointed out by others [23], it is remarkable how simple closure schemes in real space yield so much more information than their counterparts in the spectral domain.

## ACKNOWLEDGMENTS

G.K. acknowledges support from the National Science Foundation (NSF-AGS-1102227 and NSF-EAR-1344703) and the US Department of Energy through the Office of Biological and Environmental Research Terrestrial Carbon Processes program (DE-SC0006967 and DE-SC0011461).

- 
- [1] R. Hill, *J. Fluid Mech.* **88**, 541 (1978).
  - [2] J. R. Herring, D. Schertzer, M. Lesieur, G. R. Newman, J. P. Chollet, and M. Larcheveque, *J. Fluid Mech.* **124**, 411 (1982).
  - [3] G. Falkovich, *Phys. Fluids* **6**, 1411 (1994).
  - [4] S. Saddoughi and S. Veeravalli, *J. Fluid Mech.* **268**, 333 (1994).
  - [5] D. Lohse and A. Müller-Groeling, *Phys. Rev. Lett.* **74**, 1747 (1995).
  - [6] D. Lohse and A. Müller-Groeling, *Phys. Rev. E* **54**, 395 (1996).
  - [7] W. Dobler, N. E. L. Haugen, T. A. Yousef, and A. Brandenburg, *Phys. Rev. E* **68**, 026304 (2003).
  - [8] A. G. Lamorgese, D. A. Caughey, and S. B. Pope, *Phys. Fluids* **17**, 015106 (2005).
  - [9] A. Moene and A. van Dijk, in *The 17th Symposium on Boundary Layers and Turbulence* (American Meteorological Society (AMS), San Diego, CA, 2006), p. 5.
  - [10] J. Meyers and C. Meneveau, *Phys. Fluids* **20**, 065109 (2008).
  - [11] U. Frisch, S. Kurien, R. Pandit, W. Pauls, S. S. Ray, A. Wirth, and J.-Z. Zhu, *Phys. Rev. Lett.* **101**, 144501 (2008).
  - [12] T. Ishihara, T. Gotoh, and Y. Kaneda, *Annu. Rev. Fluid Mech.* **41**, 165 (2009).
  - [13] W. J. T. Bos, L. Chevillard, J. F. Scott, and R. Rubinstein, *Phys. Fluids* **24**, 015108 (2012).
  - [14] L. M. Smith and W. C. Reynolds, *Phys. Fluids A* **3**, 992 (1991).
  - [15] T. Watanabe and T. Gotoh, *New J. Phys.* **6**, 40 (2004).
  - [16] D. Donzis and K. Sreenivasan, *J. Fluid Mech.* **657**, 171 (2010).
  - [17] U. Frisch, S. S. Ray, G. Sahoo, D. Banerjee, and R. Pandit, *Phys. Rev. Lett.* **110**, 064501 (2013).
  - [18] K. Verma and D. Donzis, *J. Physics A* **40**, 4401 (2007).
  - [19] F. Champagne, C. Friehe, and J. LaRue, *J. Atmos. Sci.* **34**, 515 (1977).
  - [20] R. Williams and C. Paulson, *J. Fluid Mech.* **83**, 547 (1977).
  - [21] H. L. Grant, B. A. Hughes, W. M. Vogel, and A. Moilliet, *J. Fluid Mech.* **34**, 423 (1968).
  - [22] T. V. Kármán and L. Howarth, *Proc. R. Soc. A* **164**, 192 (1938).
  - [23] P. Davidson, *Turbulence: An Introduction for Scientists and Engineers* (Oxford University Press, New York, 2004), p. 651.
  - [24] F. Thiesset, R. A. Antonia, L. Danaila, and L. Djenidi, *Phys. Rev. E* **88**, 011003 (2013).
  - [25] G. Batchelor, in *The Theory of Homogeneous Turbulence* (Cambridge University Press, London, 1953), p. 197.
  - [26] U. Frisch, in *Turbulence: The Legacy of A. N. Kolmogorov* (Cambridge University Press, New York, 1995), p. 296.
  - [27] A. M. Obukhov, *Dokl. Akad. Nauk. SSSR* **67**, 643 (1949).